

# The $\Lambda(1405)$ from Lattice QCD: Something about determining the Finite-volume Spectra

John Bulava, Bárbara Cid-Mora<sup>1,2</sup>, Andrew D. Hanlon, Ben Hörz, Daniel Mohler, Colin Morningstar, Joseph Moscoso, Amy Nicholson, Fernando Romero-López, Sarah Skinner, André Walker-Loud

<sup>1</sup>GSI Helmholtzzentrum für Schwerionenforschung GmbH, Darmstadt, Germany

<sup>2</sup>Technische Universität Darmstadt &, Germany

## ABSTRACT

Hadronic scattering amplitudes determined in Lattice QCD using Lüscher's formalism depend crucially on the finite-volume energy spectrum. Due to the critical dependence of the amplitudes on the spectra, this work presents some of the technical details of determining such spectra for the scattering amplitude of the coupled-channel  $\pi\Sigma - \bar{K}N$  [1, 2]. Finally, the results exhibit a two-pole structure for the  $\Lambda(1405)$ , a virtual bound state below the  $\pi\Sigma$  threshold and a resonance pole right below the  $\bar{K}N$  threshold.

## Ensemble details

The coupled channel  $\pi\Sigma - \bar{K}N$  scattering amplitudes in the  $\Lambda(1405)$  region and below  $\pi\pi\Lambda$  were explored using a single ensemble of gauge configurations ( $N_f = 2 + 1$ ) [4].

$a[\text{fm}]$	$(L/a)^3 \times T/a$
0.0633(4)(6)	$64^3 \times 128$

Table 1. Lattice extent and Lattice spacing of the D200 ensemble. Pion mass  $m_\pi \approx 200$  MeV, and kaon mass  $m_K \approx 487$  MeV.

The D200 ensemble of QCD gauge configurations generated by CLS was employed.

- Mass-degenerate  $u, d$ -quarks heavier than physical, and  $s$ -quark lighter than physical.
- Tree-level improved Lüscher-Weisz gauge action.
- Non-pert  $O(a)$ -improved Wilson fermion action.
- Open temporal boundary conditions.

## Correlator analysis

→ Correlation functions ( $C(t)$ ) were built using single and multihadron operators:

$\Lambda, \pi\Sigma$  and  $\bar{K}N$

(See Ref. [2] for the complete list)

→ Autocorrelation was studied using the computation of the pion mass (see Fig. 1) including binning and number of Bootstrap samples, which were chosen as  $N_{\text{bin}} = 10$  (binning) and  $N_B = 800$  (number Bootstrap samples).

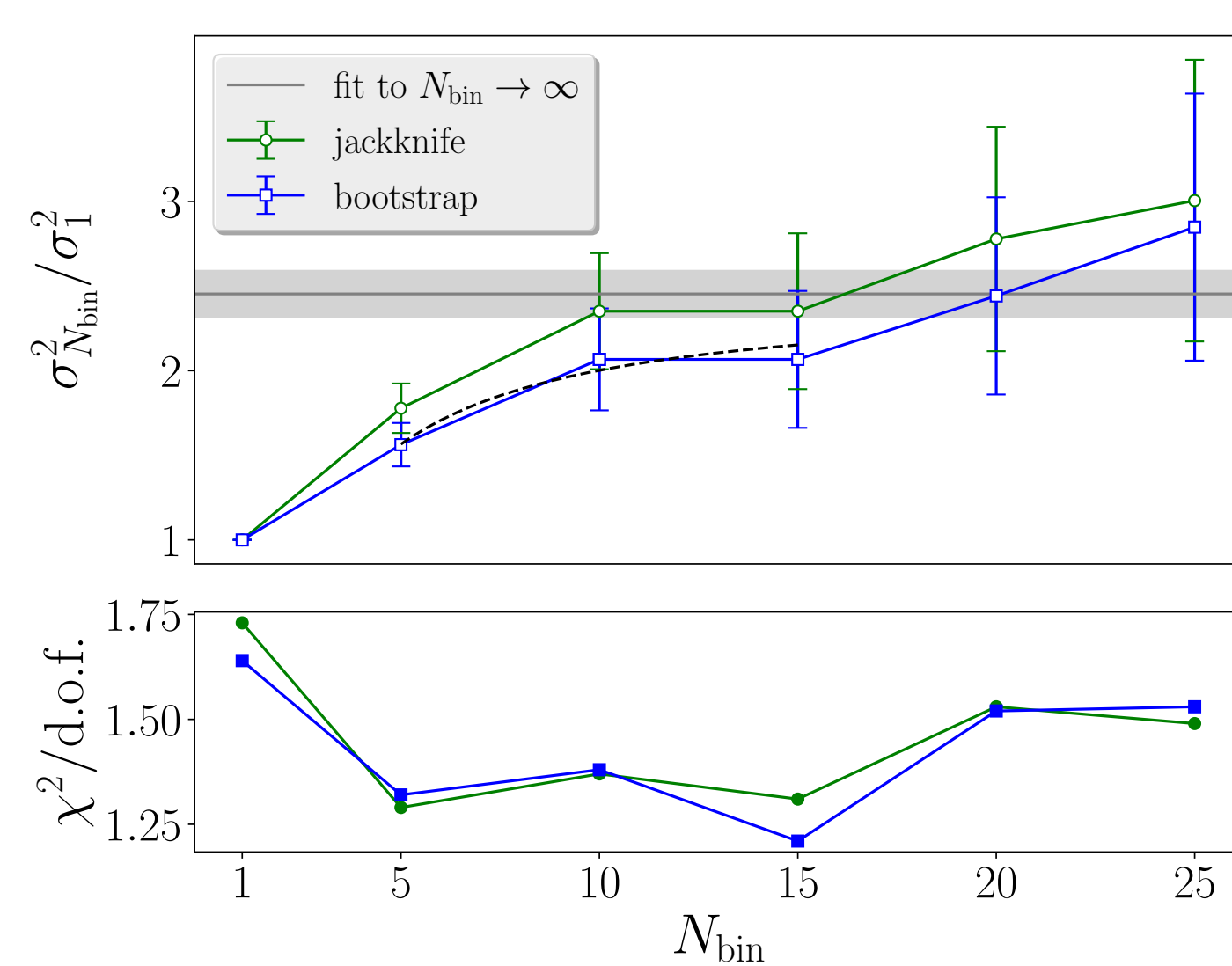


Figure 1. (Top) Ratios of variances for fits to  $m_\pi$  for different bin sizes. (Bottom) Correlated- $\chi^2$  of two-exponentials fit to  $m_\pi$  versus  $N_{\text{bin}}$ .

## Diagonalization of correlation matrices

The extraction of the finite-volume energy spectrum was done using the variational method through two independent analyses (more details of this method in Ref. [3, 5, 6]).

$$C(t_d)\vec{v}_n(t_0, t_d) = \lambda_n(t_0, t_d) C(t_0)\vec{v}_n(t_0, t_d), \quad (\text{GEVP})$$

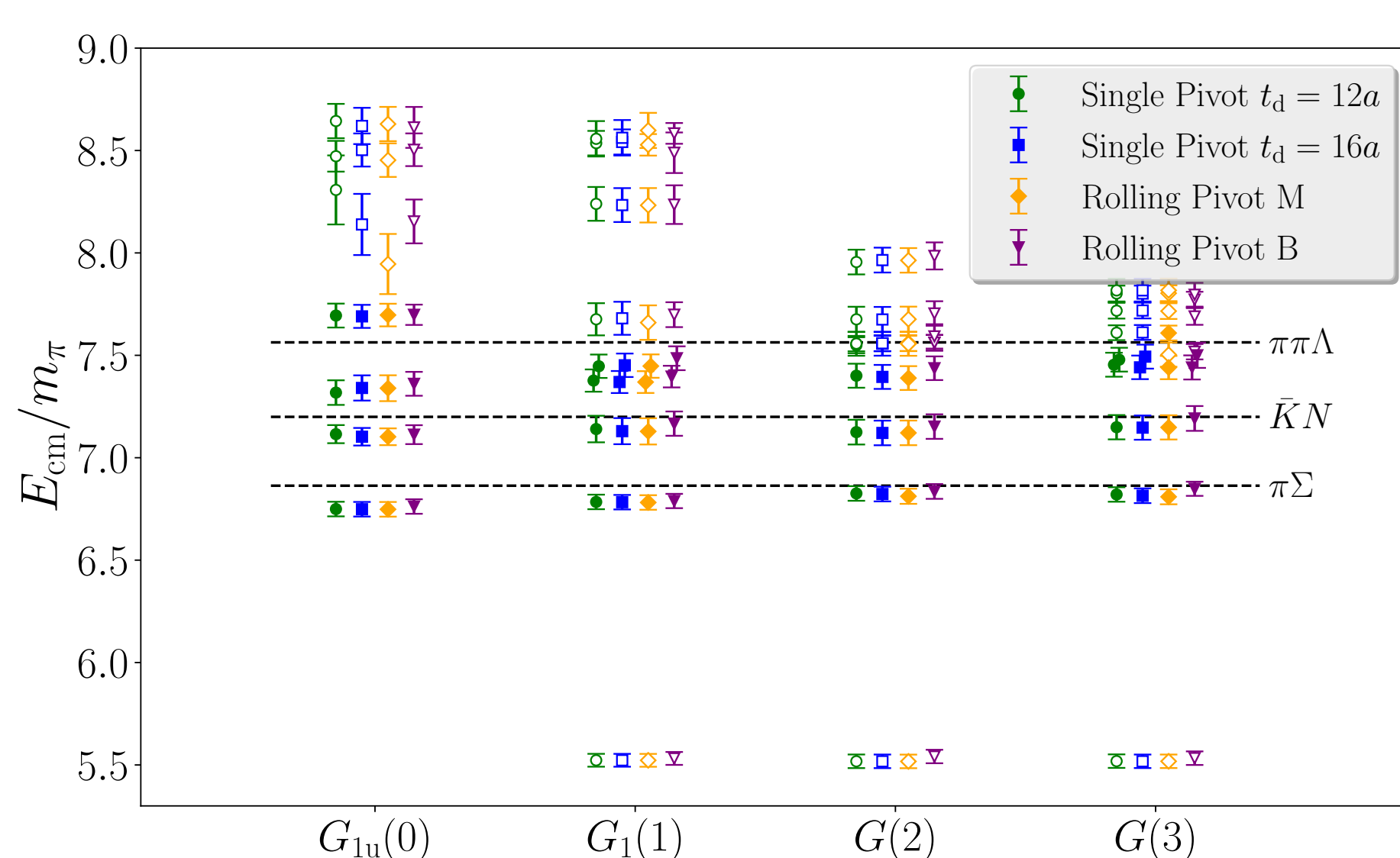


Figure 2. Center-of-mass finite-volume energy spectra under variation of diagonalization method and diagonalization time ( $t_d$ ) for single pivot method.

$t_0$ : metric time.  
 $t_d$ : diagonalization time.  
 $\lambda_n$ : eigenvalues.

The differences of both methods are:

- ▷ **Single Pivot**: a single choice of  $t_0$  and  $t_d$  is used to rotate  $C(t)$  for all times  $t$ .
- ▷ **Rolling Pivot**: a single choice of  $t_0$  is used, but  $C(t)$  is rotated at all times  $t_d = t$ .

## Finite-volume energies

Single hadrons and correlator matrices were treated slightly different.

- + **Single Hadrons**: Diverse fit models were used, one- and two-exponentials fits, and geometric-exp series. Final results for single hadron masses are shown in Table 2.

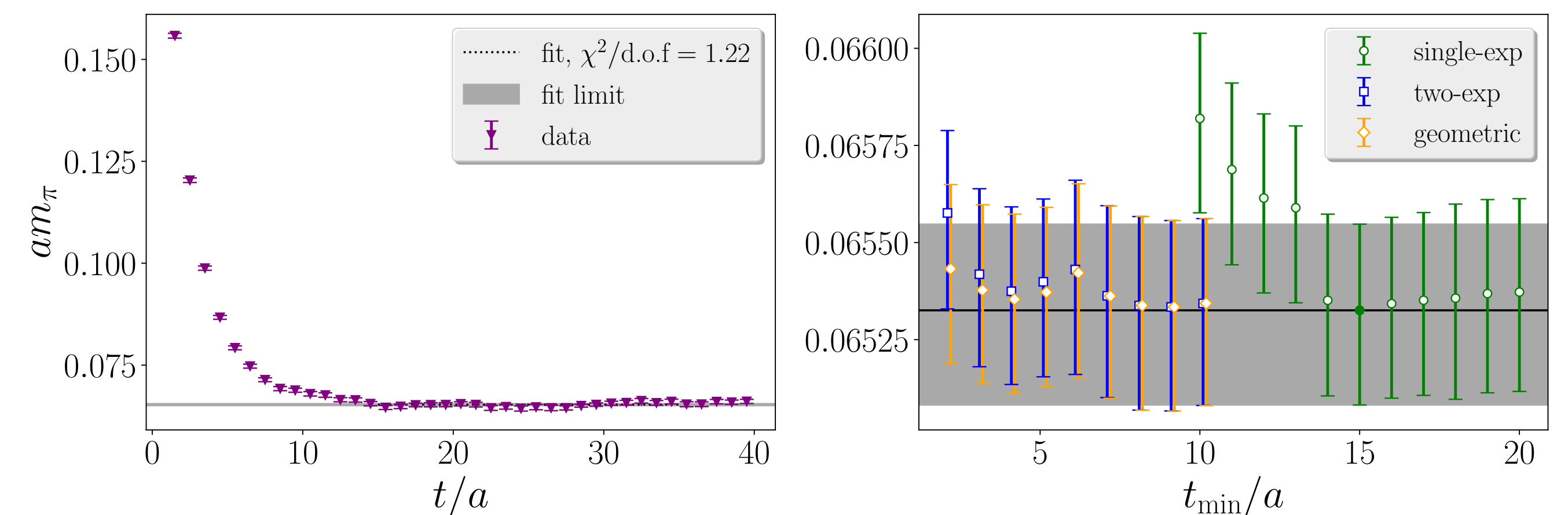


Figure 3. Pion mass: (left column) Effective energy and its final fit result; (right column) Different fit models versus variation of  $t_{\text{min}}$ .

$am_\pi$	0.06533(25)	$am_\Lambda$	0.3634(14)	$am_K$	0.15602(16)
$am_\Sigma$	0.3830(19)	$am_N$	0.3143(37)	$am_\Xi$	0.41543(96)

Table 2. Summary of hadron masses in Lattice units.

- + **GEVP Eigenvalues**: Additionally the one-exponential fit to a ratio of correlators was included for the GEVP eigenvalues.

$$R_n(t) = \frac{\lambda_n(t)}{C_A(\mathbf{d}_A^2, t)C_B(\mathbf{d}_B^2, t)}$$

where  $(A, B) = (\pi, \Sigma)$  or  $(\bar{K}, N)$ , and  $\mathbf{d}_{A,B}^2$  are:

$$E_n^{\text{non-int}} = \sqrt{m_A^2 + \left(\frac{2\pi\mathbf{d}_A^2}{L}\right)^2} + \sqrt{m_B^2 + \left(\frac{2\pi\mathbf{d}_B^2}{L}\right)^2}$$

$E_n^{\text{non-int}}$ : non-interacting energy sum close to the stationary state energy. This ratio allowed us to determine the energy interaction shift  $a\Delta E$  whilst taking advantage of noise-cancellation. The lab-frame energy was obtained:

$$aE_n^{\text{lab}} = a\Delta E + aE_n^{\text{non-int}}$$

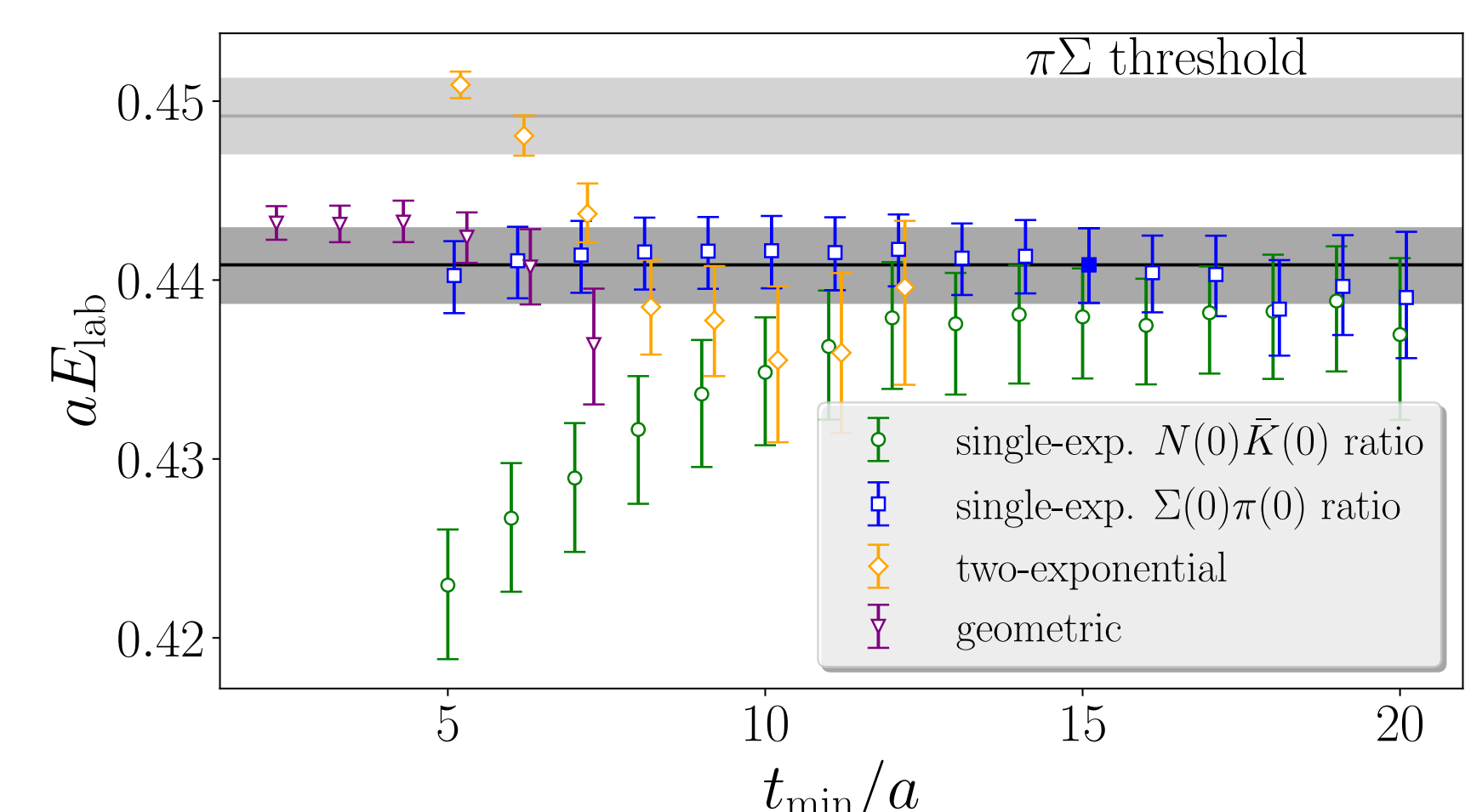


Figure 4. Stability plot of energy fit for the lowest level of the  $G_{1u}$  irrep using diverse fit models, including two different non-interacting ratios.

## Conclusion

- ✓ The finite-volume spectra was extracted reliably using different methods, which included variations of the implementation of the GEVP and a variety of fit models.
- ✓ The results from all mentioned approaches were consistent along the analysis, and the set of energy levels showed good agreement between them (see Fig. 5).
- ✓ Subsequently this spectra was used as an input to compute Scattering amplitudes using Lüscher's formalism (see parallel talk by Fernando Romero-López).

## References

- [1] J. Bulava, B. Cid-Mora, A. D. Hanlon, B. Hörz, D. Mohler, C. Morningstar, J. Moscoso, A. Nicholson, F. Romero-López and S. Skinner, A. Walker-Loud. "The two-pole nature of the  $\Lambda(1405)$  from Lattice QCD." [arXiv:2307.10413 [hep-lat]].
- [2] J. Bulava, B. Cid-Mora, A. D. Hanlon, B. Hörz, D. Mohler, C. Morningstar, J. Moscoso, A. Nicholson, F. Romero-López and S. Skinner, *et al.* [arXiv:2307.13471 [hep-lat]].
- [3] J. Bulava, A. D. Hanlon, B. Hörz, C. Morningstar, A. Nicholson, F. Romero-López, S. Skinner, P. Vranas and A. Walker-Loud, "Elastic nucleon-pion scattering at  $m_\pi = 200$  MeV from lattice QCD," Nucl. Phys. B **987** (2023), 116105 doi:10.1016/j.nuclphysb.2023.116105 [arXiv:2208.03867 [hep-lat]].
- [4] M. Bruno, D. Djukanovic, G. P. Engel, A. Francis, G. Herdoiza, H. Horch, P. Korczyk, T. Korzec, M. Papinutto and S. Schaefer, *et al.* JHEP **02** (2015), 043 doi:10.1007/JHEP02(2015)043 [arXiv:1411.3982 [hep-lat]].
- [5] B. Blossier, M. Della Morte, G. von Hippel, T. Mendes and R. Sommer, JHEP **04** (2009), 094 doi:10.1088/1126-6708/2009/04/094 [arXiv:0902.1265 [hep-lat]].
- [6] C. Michael and I. Teasdale, Nucl. Phys. B **215** (1983), 433-446 doi:10.1016/0550-3213(83)90674-0

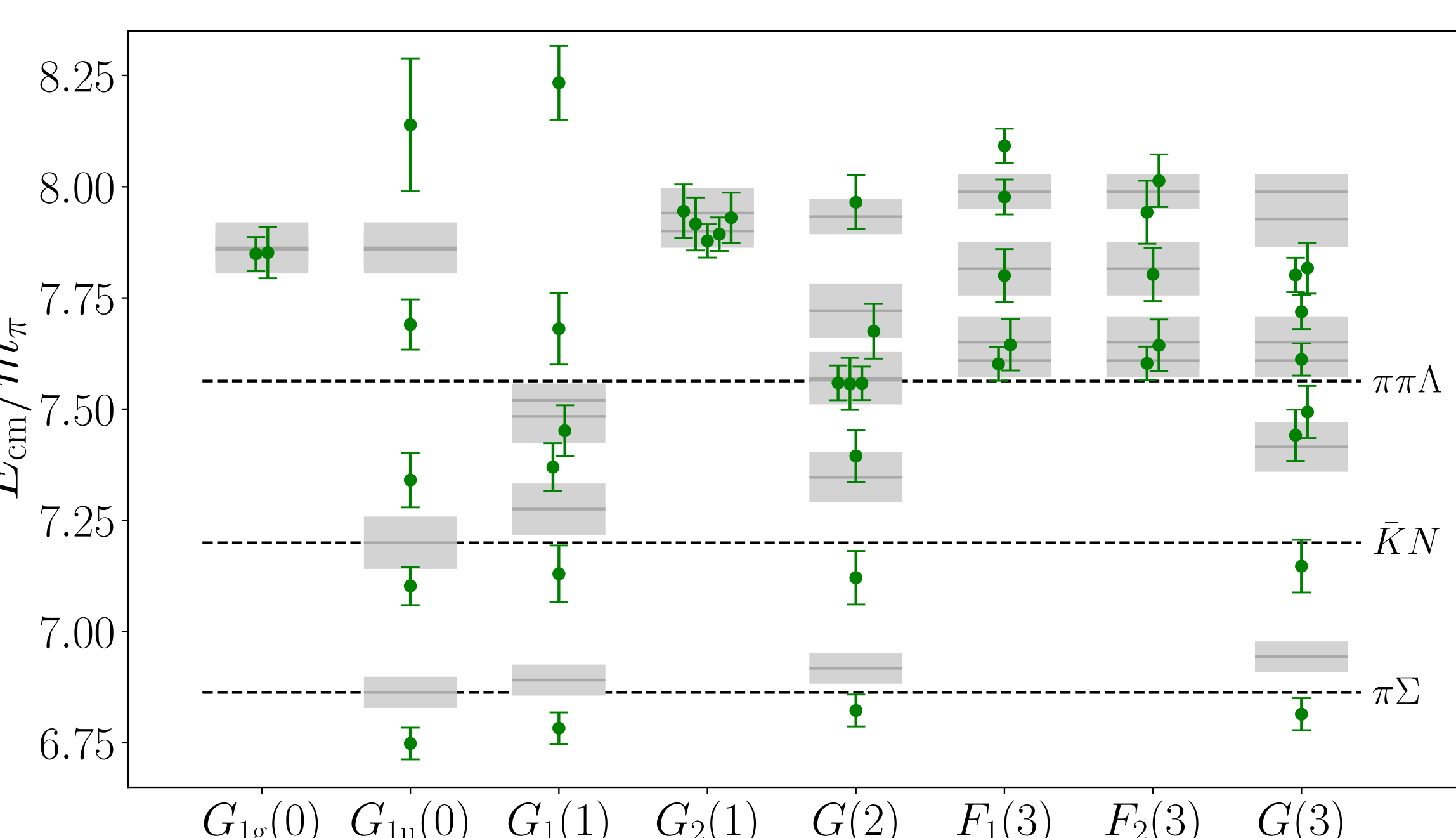


Figure 5. Final results: (Green) Finite-volume stationary-state spectrum in the center-of-mass frame. (Gray) Locations of energy sums for non-interacting hadrons.